Published in Sustainable Cities and Society with doi: 10.1016/j.scs.2024.105878

Robust Day-ahead Scheduling of Cooperative Energy Communities Considering Multiple Aggregators

Marcos Tostado-Véliz[1], Juan S. Giraldo[2], Daniel Icaza Álvarez[3], Carlos Cruz[4], Francisco Jurado[1,*]

1. Department of Electrical Engineering, University of Jaén, 23700 EPS Linares, Jaén, Spain (e-mail: mtostado@ujaen.es (M.T.-V.), fjurado@ujaen.es (F.J.)).
2. Energy Transition Studies Group, Netherlands Organisation for Applied Scientific Research (TNO), Amsterdam, 1043 NT, The Netherlands (e-mail: juan.giraldo@tno.nl).
3. Postgraduate Unit, Department of Electrical Engineering, Catholic University of Cuenca, 010107 Cuenca, Ecuador (e-mail: dicazaa@ucacue.edu.ec)
4. Department of Electronics, University of Alcalá, Alcalá de Henares, 28805, Spain (e-mail: carlos.cruzt@uah.es)

* Correspondence: fjurado@ujaen.es

Abstract. Future cities must play a vital role in reducing energy consumption and decarbonizing the electricity sector, thus evolving from passive structures towards more efficient smart cities. This transition can be facilitated by energy communities. This emerging paradigm consists of collectivizing a set of residential installations equipped with onsite renewable generators and storage assets (i.e., prosumers), which can eventually share resources to pursue collective welfare. This paper focuses on cooperative communities, where prosumers share resources without seeking selfish monetary counterparts. For this kind of scheme, a novel management structure based on multiple aggregators is proposed. This paradigm preserves users' confidential features while allowing them to extract the full potential of their assets. To efficiently manage the variety of assets available under uncertainty, an adaptive robust day-ahead scheduling model is developed, which casts as a solvable and portable Mixed Integer Linear Programming framework. The new proposal concerns uncertain generation and demand using a polyhedral representation of the uncertainty set. A case study is conducted to validate the developed model, showing promising results. Moreover, different results are obtained and analysed. Finally, it is worth remarking on how the level of robustness impacts the collective bill, incrementing it by 75 % when risk-averse conditions are assumed. In addition, the role of storage assets under pessimistic conditions is remarked, pointing out that these assets rule the scheduling plan of the community instead of renewable generators.

Keywords. Energy community; Energy Storage; Robust optimization; Uncertainty.

Nomenclature

Indices (sets)	
$j(\mathcal{J})$	Prosumer
$t(\mathcal{T})$	Time
a	Referred to a parameter passed to an aggregator
$c(\mathcal{C})$	Shiftable appliance
Θ	Allowable time windows for appliances and electric vehicles
Superscripts	
Net	Net demand
NF/F	Non-flexible/flexible demand
PV	Photovoltaic
$Shift$	Shiftable appliances
$Air, in/out$	Indoor/outdoor air
$HVAC$	Heating-ventilation-air conditioner system
sp/db	Setpoint/dead-band
$W, h/c$	Hot/cold water
EWH	Electric water heater
$ES, ch/dch$	Energy storage in charging/discharging mode
Bat	Batteries
EV	Electric vehicle
$\overline{(\cdot)}/\underline{(\cdot)}$	Maximum/minimum value
$\widetilde{(\cdot)}/\widetilde{\widetilde{(\cdot)}}$	Forecasted/calculated value
Parameters	
ϑ	Solar irradiance [kW/m²]
θ	Temperature [ºC]
DC	Duty cycle of a shiftable appliance [hours]
Δt	Time step [hours]
A/B	Thermal characteristics of the building [-/(kW/ºC)]
COP	Coefficient of performance [-]
C	Thermal capacity [kWh/ºC]
R	Equivalent thermal resistance [kWh/ºC]
v	Volume [gal]
η	Efficiency [pu]
DOD	Depth-of-discharge [%]
e2P	Energy-to-power ratio [hours]
Γ	Uncertainty budget [-]
π	Energy cost [$/kWh]
M	Large positive number [-]
δ	Parameter that relates purchasing and selling energy prices ($0 \leq \delta < 1$)
Variables	
p	Power [kW]
y	Commitment statuses [binary]
ε	Energy [kWh]
λ	Dual variable associated to equality constraints [-]

$\underline{\mu}, \overline{\mu}$	Dual variable associated to inequality constraints [-]
$\underline{z}, \overline{z}$	Dummy variable to linearize complementarity terms [binary]
Variables (vector notation)	
$\boldsymbol{x}$	Vector of primal continuous variables
$\boldsymbol{y}$	Vector of primal binary variables
$\boldsymbol{\lambda}$	Vector of dual variables associated to equality constraints
$\underline{\boldsymbol{\mu}}, \overline{\boldsymbol{\mu}}$	Vector of dual variable associated to inequality constraints
$\underline{\boldsymbol{z}}, \overline{\boldsymbol{z}}$	Vector of dummy variable to linearize complementarity terms

1 - Introduction

1.1 - Context and motivation

Residential sector contributes with a large share of global electricity consumption, thus contributing notably to global warming with dramatic effects on population lifestyle [1]. To reduce the negative effects of global warming, governmental entities are promoted measures to decarbonize the energy sector [2], such as promote the use of renewable generators. The increasing penetration of renewable sources and wide adoption of demand response initiatives are driving the transition of power distribution systems from passive to active networks [3]. This transition poses significant challenges for systems operators such as duck curves, bidirectional power flows and privacy concerns [4]. Under this paradigm, a growing interest for local energy communities (LECs) has been observed in recent years. According to [5], LECs aim at collectivizing citizen energy actions pursuing different economic, environmental and social benefits.

The optimal exploitation of available resources as well as coordination of the different agents involved in a LEC require the implementation of energy management systems [6]. Such tools differ from conventional energy management strategies in a variety of aspects, being primordial to pay attention at privacy concerns, impact of uncertainties and peer-to-peer (P2P) energy sharing. This paper focuses on this issue.

1.2 - Energy management in LECs: state-of-the-art

According to [7], a LEC can be understood as a group of a few prosumers that are eventually willing to share energy resources. Under this definition, energy management or different dispatch strategies for LECs were firstly studied in various works [8, 9]. However, this very first works rather focused on introducing basic concepts or describing the necessary communication infrastructures for P2P power sharing within communities. More comprehensive works have been developed since 2019, focusing on a variety of aspects.

Broadly, energy management in LECs can be performed in a centralized, decentralized or distributed way. Centralized frameworks are the most logical option and ensure that global objectives are optimized. In such paradigms, a central operator is responsible of collecting information from prosumers and decide the optimal scheduling strategy consequently. Nevertheless, this kind of frameworks reveal privacy data as prosumers need to share confidential information with the coordinator. The simplest methodologies based on centralized scheduling assume that the coordinator has complete access to information [10-12]. This approach, although ensure reachability of collective goals, entail clear privacy concerns as some users may be reluctant to share confidential information. More sophisticated approaches present multi-layer structures [13-15], in which information from prosumers is not fully shared but flexibility can be leveraged yet. Within this category, there exists other methodologies rather focused on other secondary aspects. For instance, reference [16] presents a game-based approach to achieve consensus among prosumers, whereas [17] is rather focused on storage sharing.

On the other hand, distributed algorithms ensure privacy of users as the energy management decisions are taken collectively in a distributed fashion. Among the existing distributed algorithms, the alternating direction of multipliers method has been successfully applied in cooperative energy communities [18, 19]. Although this approach ensures that users' privacy is completely preserved, its computational tractability may be challenging due to two issues: 1) the solution is obtained iteratively solving a collection of optimization problems; and 2) the optimization problem results quadratic, for which off-the-shelf solvers are not frequently available. Moreover, the alternating direction of multipliers may unintentionally benefit to large consumers/generators. This situation, although unlikely in residential communities, may occur in LECs involving non-residential users like parking lots, commercial buildings or large storage facilities. Alternatively, a hierarchical energy management framework was proposed in [20], which ensures privacy since only prosumers' net load profiles are communicated to a central entity. This approach is similar to the multi-layer frameworks in [13-15] but ensuring total privacy. However, as only load profiles are shared, opportunities provided by flexible devices as controllable appliances and electric vehicles (EVs) could not be fully exploited.

Uncertainty modelling is another important aspect in energy communities. In LECs, uncertainties may be brought from different sources such as demand, renewable generation or energy prices. However, as LECs are normally small-scale entities, volatility in prices can be diminished by agreeing tariffs with a retailer [7]. Surprisingly, it is a underaddressed issue in LECs. In [19], the day-ahead scheduling problem is modelled using scenarios, which aim at capturing the volatility of loads and renewable generation. Although this approach is simple and preserves the model linear, it presents two important issues: on the one hand, stochastic approaches are probabilistic rather than robust, so that the problem is not solved for the worst-case realization of uncertainties. On the other hand, computational burden of this kind of problems dramatically increases with the number of scenarios considered [21]. Such issues are partially solved by hybridizing scenarios with robust-based approaches like interval notation [13] and information gap decision theory (IGDT) [14]. Furthermore, a day-ahead scheduling tool purely based on IGDT was proposed in [15] for LECs. However, such approaches do not ensure robust solution as the worst-case realization of uncertainties is approached rather than looked for.

Lastly, it is worth analysing which capabilities are actually shared within the community environment. Indeed, the most basic community structure is devoted on P2P exchanges among prosumers. Nevertheless, most of the studied methodologies pay special attention to share flexibility provided by smart appliances. Fully capabilities of such devices can be effectively leveraged in centralized approaches with fully information access. However, when privacy concerns are taken into account, total flexibility provided by prosumers can be hidden, thus hindering the possibility of reaching collective goals [13-15, 20]. Nevertheless, prosumers can offer further capabilities within a community structure, especially storage capacity. Such feature can be provided by either installing batteries at homes or enabling bidirectional power flow from EVs. For the former case, auction-based approaches have been successfully investigated [17], while only some handful works have already considered the storage capability provided by EVs [13]. Storage sharing in LECs is an open topic that might present important difficulties to be implanted in real cases. However, its implications are worth to be investigated. For the sake of simplicity, Table 1 collects the main features of the selected literature and gives a comparison with the present work.

Table 1 - A summary of the studied literature

Ref.	Model	Uncertainty	Shared capabilities	
			Flexibility	Storage
[7]	MCP	Risk-averse	Yes	No
[10]	QP	No	Yes	Yes
[11]	Heuristic	No	No	No
[12]	MILP	No	Yes	Yes
[13]	MILP-QP	Hybrid	Yes	Yes
[14]	MILP	Hybrid	No	Yes
[15]	MILP	IGDT	Yes	Yes
[16]	LP	No	Yes	Yes
[17]	MILP	No	No	Yes
[18]	QP	No	No	No
[19]	QP	Stochastic	No	No
[20]	MILP	No	Yes	Yes
Present	MILP	Robust	Yes	Yes

MCP: mixed complementarity problem
QP: quadratic programming
MILP: mixed-integer linear programming
LP: linear programming

1.3 - Contributions

The main research focus lies on the uncertainty modelling in LECs. It was previously discussed that there exists an important gap in this field. Actually, to the best of our knowledge, any of the studied references can be conceived as a robust approach. Existing works mainly rely on scenario-based techniques that do not ensure robustness of the solution. To this end, an adaptive robust formulation of the day-ahead scheduling problem in LECs is proposed. The new methodology is based on other robust-based approaches already applied to different well-known problems [22, 23], and ensures that the worst-case realization of uncertainties is revealed and the scheduling decisions are taken in consequence.

The present work also concerns about privacy issues in communities. To partially preserve the privacy of prosumers while their flexibility is fully leveraged, an innovative community structure based on multi-purpose aggregators is proposed. This way, the community members only share innocuous information with the aggregators and not with the coordinator or other prosumers. In this regard, the role of three emerging agents in LECs is explored: the net demand aggregator, who is responsible on aggregating net load profiles and communicate importable and exportable power from prosumers; the flexibility aggregator, who aggregates flexible demand capabilities from household devices; and the storage aggregator, who concerns about both stationary batteries and EV on-board storage systems to provide storage capability in the community. For simplicity, the main contributions of this work are summarized below:

- Developing an adaptive robust day-ahead scheduling tool for cooperative ECs accounting for uncertainties in demand and renewable generation.
- Proposing an innovative community structure based on multi-purpose aggregators with the aim of exploiting fully flexibility from users while their privacy is partially preserved. To this end, mathematical modelling of each aggregator is derived.

In the rest of this paper, Section 2 comments the proposed community layout as well as the role of each agent together with some plausible assumptions. Section 2 also presents the mathematical modelling of the three proposed aggregators and derives the robust day-ahead scheduling model for the considered community. Section 3 presents some numerical results and discussion. Finally, the paper is concluded with Section 4.

2 – Materials and methods

2.1 – Community structure

Fig. 1 depicts a schematic representation of the proposed community structure based on multi-purpose aggregators. A group of prosumers constitute the core of the community. Each prosumer is assumed to actively partake in the community, for which different smart devices are available to enable flexible consumption. In particular, it is assumed that each household owns rooftop photovoltaic (PV) units, stationary batteries, EV charger (with bidirectional power flow enabled) and a set of controllable (flexible) and non-controllable (non-flexible) appliances. In the former case, it is distinguished between shiftable and thermostatically controlled appliances [24]. The first encompasses some characteristic devices whose operation can be shifted throughout the day for convenience, but respecting some preferences of users. The thermostatically controlled appliances are temperature-based devices within which one can find heating-ventilation air conditioner (HVAC) systems and electric water heaters (EWHs).

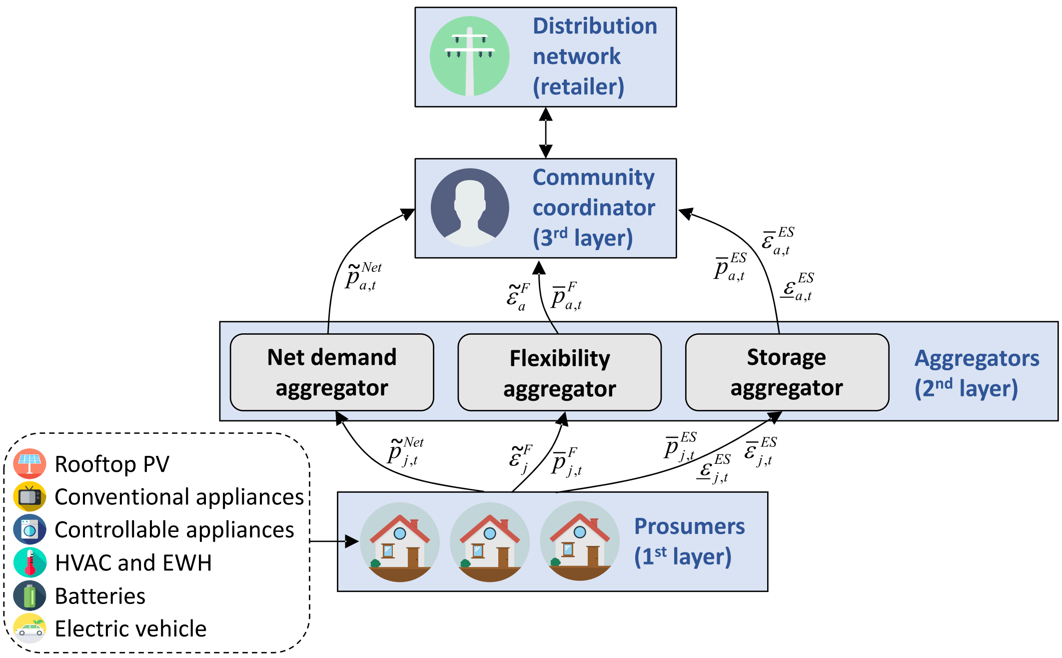

Fig. 1 - Schematic representation of the community under study

Daily, each prosumer communicates to each aggregator some necessary information. Assuming that each prosumer can forecast their own net demand (non-flexible demand minus PV production) with acceptable accurateness, such profiles are sent to the net demand aggregator, who decomposes them into non-flexible demand and local generation (through PV units). The flexibility aggregator receives two values daily. Firstly, the total energy required by flexible devices (shiftable and thermostatically controlled appliances) denoted by $\tilde{\varepsilon}_j^F$, which gives an idea about how much energy will be demanded by flexible appliances throughout the day. Secondly, the instantaneous maximum power that flexible appliances can dispatch given by $\overline{p}_{j,t}^F$. These last value accounts for two features of controllable appliances. On the one hand, each appliance is assumed to present an upper bound in the power that can absorb, normally fixed by rated values. On the other hand, controllable appliances are assumed to be scheduled within predefined time windows describing preference users [24]. Likewise, the storage aggregator receives the maximum power dispatchable to storage units given by $\overline{p}_{j,t}^{ES}$, but also the available storage bounds denoted by $\underline{\varepsilon}_{j,t}^{ES}$ and $\overline{\varepsilon}_{j,t}^{ES}$. Note that storage bounds are a function of the time in order to capture the availability of EVs.

After receiving all the relevant information, individual profiles are aggregated and send to the community coordinator, who is responsible of deciding the day-ahead scheduling plan for the entire community. This task is performed on the basis of energy prices previously agreed with a local retailer and targets minimizing the collective bill. After deciding the power dispatched, it is communicated to each aggregator, who disaggregate the different profiles to allocate power signals among prosumers. This task can be performed under different logical rules. However, this step is out of scope of the present work and the reader is referred to [11] for further information.

One important feature of the proposed community structure is that very few information is transferred to the community operator (see the symbols included in Fig. 1). Actually, this agent receives aggregated information so that individual features of prosumers are not revealed. In this sense, it is worth noting that aggregators only perform summation of profiles, so that these agents may be simply data hubs, thus hiding the information to other people. This way, individual privacy of users is ensured.

It is assumed that prosumers collaborate within the community in a cooperative way, so that minimization of the collective bill is the unique objective pursued by users. This way, prosumers do not pay/are not paid by P2P exchanges, assuming that power sharing in the community always leads to minimize the entire community cost [19]. On the other hand, it is assumed that prosumers have some smart capability in order to firstly forecast their own consumption/generation, and secondly to schedule their own assets responding to signals received from the aggregators. In this sense, the energy management of each building is out of scope of the present paper, being the reader referred to the rich existing literature [24, 25]. In this regard, it is worth noting that home energy management is not performed before sending information to aggregators. Instead, it is assumed that this step is performed after receiving power signals from aggregators once the community operator has decided the day-ahead scheduling plan for the community. Lastly, electrical network is not considered owing to homes are assumed to be located near each other, as customary in LECs [7, 19].

2.2 - Aggregators modelling

Herein, the mathematical model of each aggregator described in Section 2.1 is presented. Note that the models presented here involve prosumers and aggregators actuation. In such a case, it is intended that prosumers should prepare their own information in adequate format for aggregators in order to preserve their privacy. Moreover, expected value of uncertain parameters are denoted by tilde $(\tilde{\cdot})$. How these parameters are treated is discussed in Section 2.3.2.

2.2.1 - Net demand aggregator

The net demand aggregator receives daily net demand from prosumers, who must forecast it in advance. Assuming that prosumers can easily forecast weather parameters such as solar irradiance and temperature, the simplified PV panel model (1) [24] can be used to estimate the PV generation.

$$\tilde{p}_{j,t}^{PV} = \overline{p}_j^{PV} \cdot \left(0.2 \cdot \tilde{\vartheta}_t + 0.024 \cdot \tilde{\theta}_{j,t}^{Air,out} \cdot \tilde{\vartheta}_t\right); \forall j \in \mathcal{J} \wedge t \in \mathcal{T} \tag{1}$$

where $\mathcal{J}$ and $\mathcal{T}$ are the set of prosumers in the LEC and time intervals. On the other hand, $\tilde{p}_{j,t}^{PV}$ denotes the estimated PV potential for the j^{th} prosumer at time t, $\overline{p}_j^{PV}$ is the installed PV peak power of the j^{th} prosumer, $\tilde{\vartheta}_t$ expresses the forecasted solar irradiance at time t and $\tilde{\theta}_{j,t}^{Air,out}$ stands for the forecasted ambient temperature at time t.

Once the instantaneous PV potential of each prosumer is calculated in (1), the net demand aggregator adds up all the profiles in (2) and decomposes the aggregated demand into non-flexible demand and PV generation in (3) and (4), respectively.

$$\tilde{p}_{a,t}^{Net} = \sum_{j\in\mathcal{J}} \tilde{p}_{j,t}^{Net}\,; \forall t \in \mathcal{T} \tag{2}$$

$$\tilde{p}_{a,t}^{PV} = -\tilde{p}_{a,t}^{Net}; \forall t\colon \tilde{p}_{a,t}^{Net} < 0 \tag{3}$$

$$\tilde{p}_{a,t}^{NF} = \tilde{p}_{a,t}^{Net}; \forall t\colon \tilde{p}_{a,t}^{Net} \geq 0 \tag{4}$$

where negative demand is considered generation, the subscript a denotes aggregated values, $\tilde{p}_{j,t}^{Net}$ is the net demand of the j^{th} prosumer at time t whereas $\tilde{p}_{a,t}^{PV}$ indicates surplus generation and $\tilde{p}_{a,t}^{NF}$ denotes net consumption in the community at time t. Thus, if there exists a surplus generation in the community, $\tilde{p}_{a,t}^{PV} > 0$, while $\tilde{p}_{a,t}^{NF} > 0$ in case of net consumption. Note that net demand is inherently uncertain in the model above due to the uncertain weather parameters and non-flexible demand [7].

2.2.2 - Flexibility aggregator

Flexibility from prosumers is enabled by flexible operation of shiftable and thermostatically-controlled appliances. In the former case, assuming a fixed duty cycle (i.e. total number of hours that an appliance must work daily), each prosumer can calculate the total energy demanded by her shiftable appliances, as follows

$$\varepsilon_j^{Shift} = \sum_{j\in\mathcal{J}} \sum_{c\in\mathcal{C}_j} \frac{\mathrm{DC}_{j,c}}{\Delta t} \cdot \overline{p}_{c,j}^{Shift} \tag{5}$$

where the set $\mathcal{C}_j$ encompasses the shiftable appliances installed by the j^{th} prosumer. $\mathrm{DC}_{j,c}$ denotes the duty cycle of the c^{th} shiftable appliance installed by the j^{th} prosumer (in hours), Δt is the time step and $\overline{p}_{c,j}^{Shift}$ is the rated power of the c^{th} shiftable appliance installed by the j^{th} prosumer. As seen, (5) basically calculates the total energy daily demanded by the shiftable appliances in the community and aggregate them to calculate ε_j^{Shift}, which is sent to the flexibility aggregator.

The power scheduled for shiftable appliances is limited by their rated power (in other words, an appliance cannot consume more power than its rated value). Thus, assuming that each shiftable appliance is only operable within some time slots (i.e. the preferable time windows Θ_c^{Shift}), the maximum instantaneous power assigned to shiftable devices is given by

$$\overline{p}_{j,t}^{Shift} = \sum_{j\in\mathcal{J}} \sum_{\substack{c\in\mathcal{C}_j \\ t\in\Theta_c^{Shift}}} \overline{p}_{c,j}^{Shift} ; \forall t \in \mathcal{T} \tag{6}$$

HVAC is devoted on maintaining the indoor temperature within acceptable margins characterized by a set-point temperature $\theta_j^{HVAC,sp}$ and a dead-band term $\theta_j^{HVAC,db}$, so that the instantaneous indoor temperature should be kept within the range $\left[\theta_j^{HVAC,sp} - \theta_j^{HVAC,db}, \theta_j^{HVAC,sp} + \theta_j^{HVAC,db}\right]$. Thus, assuming that the ambient temperature can be easily predicted, each prosumer can estimate her total HVAC consumption according to (7) and (8).

$$\Delta\tilde{\theta}_{j,t}^{Air,in} = \frac{\theta_j^{HVAC,sp} + \theta_j^{HVAC,db}}{\theta_j^{HVAC,sp}} \cdot \frac{\Delta t}{A_j^{Air,in}} \cdot \left(\tilde{\theta}_{t-1}^{Air,out} - \theta_j^{HVAC,sp}\right); \forall j \in \mathcal{J} \wedge t \in \mathcal{T} \backslash t = 1 \tag{7}$$

$$\tilde{\varepsilon}_j^{HVAC} = \frac{B_j^{Air,in} \cdot \sum_{t\in\mathcal{T}} \left|\Delta\tilde{\theta}_{j,t}^{Air,in}\right|}{\mathrm{COP}_j^{HVAC}}; \forall j \in \mathcal{J} \tag{8}$$

The thermal characteristics of the building and air impact on the functioning of HVAC devices. Such characteristics are normally characterized by a series of parameters such as the mass of air or thermal resistance of the building (see [13] for details). In this work and for easing the notation, such parameters have been gathered in the parameters A and B in the equations above.

In (7), each prosumer calculates the instantaneous deviation of the inside temperature with respect to the HVAC setpoint. Intuitively, the total energy required by HVAC to keep the thermal comfortability will be a function of (7). Indeed, the HVAC will be requested to operate always the indoor temperature deviates from the established set-point, activating the heating mode if the temperature falls below $\theta_j^{HVAC,sp} - \theta_j^{HVAC,db}$ and the cooling mode otherwise.

Note that, since dead-bands are included to avoid a frequent operation of the HVAC units, equation (7) is certainly relaxed including a term inversely proportional to the dead-band amplitude. This way, the total energy that the jth prosumer will need to maintain thermal comfort can be estimated in (8) and the value of $\tilde{\varepsilon}_j^{HVAC}$ is sent to the flexibility aggregator.

Similarly, one can calculate the total energy demanded by EWH as a function of the hot water consumption, as follows

$$\Delta\tilde{\theta}_{j,t}^{W,h} = \frac{\Delta t \cdot \left(\overline{\theta}_j^{W,h} - \theta_j^{EWH,sp}\right)}{\overline{\theta}_j^{W,h}} \cdot \left[\begin{array}{c} \theta_j^{EWH,sp} - \\ \left(\theta_j^{HVAC,sp} - \theta_j^{EWH,sp}\right) \cdot e^{\left(\frac{-\Delta t}{C^{W,h} \cdot R^{W,h}}\right)} + \\ \frac{\theta_j^{EWH,sp} \cdot \left(\overline{v}^{EWH} - \tilde{v}_{j,t}^{W,h}\right) + \theta^{W,c} \cdot \tilde{v}_{j,t}^{W,h}}{\overline{v}^{EWH}} \end{array}\right]; \forall j \in \mathcal{J} \wedge t \in \mathcal{T} \tag{9}$$

$$\tilde{\varepsilon}_j^{EWH} = \frac{\sum_{t\in\mathcal{T}}\left|\Delta\tilde{\theta}_{j,t}^{W,h}\right|}{\eta_j^{EWH}\cdot C^{w,h}} \tag{10}$$

where $\overline{\theta}_j^{W,h}$ is the maximum temperature of the EWH installed by the j^{th} prosumer, while $\theta_j^{EWH,sp}$ stands for its set-point. In (9), $C^{w,h}$ stands for the thermal capacity of hot water and $R^{W,h}$ denotes the thermal resistance of the heater. On the other hand, $\overline{v}^{EWH}$ indicates the total capacity of the heater installed by the j^{th} prosumer (in gallons) and $\tilde{v}_{j,t}^{W,h}$ the expected hot water consumption of the j^{th} prosumer at time *t*. In line with [26], it is assumed that hot water consumed is instantaneously filled with cold water, whose temperature is $\theta^{W,c}$, while η_j^{EWH} stands for the efficiency of the heater. Note that (9) assumes that indoor temperature is equal to $\theta_j^{HVAC,sp}$ or close to it, which is plausible due to the action of HVAC.

Basically, (9) is a modified version of the equations in [26], which model the thermal characteristics of the EWH. Similar to (7), equation (9) estimates the deviation of the hot water temperature with respect to the heater set-point, in order to estimate the total energy demanded by these devices in (10) and sends this value to the flexibility aggregator.

Once the energy required by shiftable appliances, HVAC and EWH has been calculated using the models above, the total energy demanded by flexible appliances can be easily calculated, as follows

$$\tilde{\varepsilon}_j^{F} = \varepsilon_j^{Shift} + \tilde{\varepsilon}_j^{HVAC} + \tilde{\varepsilon}_j^{EWH}; \forall j \in \mathcal{J} \tag{11}$$

Then, the flexibility aggregator simply adds up the energy signals of each prosumer to determine the flexible energy required by the community in (12).

$$\tilde{\varepsilon}_a^{F} = \sum_{j\in\mathcal{J}} \tilde{\varepsilon}_j^{F} \tag{12}$$

On the other hand, each prosumer can determine the maximum instantaneous power that can allocate to her own flexible devices by (13), where the rated powers of HVAC and EWH (which are assumed to be operable any time instant) are added to the value obtained in (6).

$$\overline{p}_{j,t}^{F} = \overline{p}_{j,t}^{Shift} + \overline{p}_j^{HVAC} + \overline{p}_j^{EWH}; \forall j \in \mathcal{J} \wedge t \in \mathcal{T} \tag{13}$$

Finally, the result of (13) is communicated to the flexibility aggregator, who collects profiles to determine the maximum flexible power in the community by (14).

$$\overline{p}_{a,t}^{F} = \sum_{j\in\mathcal{J}} \overline{p}_{j,t}^{F}; \forall t \in \mathcal{T} \tag{14}$$

It is worth noting that (12) is actually uncertain due to the effect of ambient temperature on the total energy demanded by thermostatically-controlled appliances.

2.2.3 - Storage aggregator

To determine the available storage capacity in the community, each prosumer determines her storage bounds by (15) and (16), which account for both stationary and on-board batteries.

$$\bar{\varepsilon}_{j,t}^{ES} = \sum_{j\in\mathcal{J}} \bar{\varepsilon}_j^{Bat} + \sum_{\substack{j\in\mathcal{J}\\ t\in\Theta_j^{EV}}} \bar{\varepsilon}_j^{EV}; \forall j \in \mathcal{J} \wedge t \in \mathcal{T} \tag{15}$$

$$\underline{\varepsilon}_{j,t}^{ES} = \sum_{j\in\mathcal{J}} \underline{\varepsilon}_{j}^{Bat} + \sum_{\substack{j\in\mathcal{J} \\ t\in\Theta_j^{EV}}} \underline{\varepsilon}_{j}^{EV}\, ; \forall j \in \mathcal{J} \wedge t \in \mathcal{T} \tag{16}$$

where $\bar{\varepsilon}_{j}^{Bat}$ and $\bar{\varepsilon}_{j}^{EV}$ denote the rated capacity of stationary batteries (e.g. Li-ion batteries) and EV batteries of the j^{th} prosumer, while $\underline{\varepsilon}_{j}^{Bat}$ and $\underline{\varepsilon}_{j}^{EV}$ give the minimum energy that must be stored in such systems to avoid their rapid degradation.

Note that, while stationary batteries are available any time instant, storage capacity provided by EVs is only accessible when vehicles are plugged. In this regard, it is assumed that each prosumer has perfect knowledge about her departure time and thus can define her own EV time window denoted by Θ_j^{EV}. This is the reason why storage bounds $\bar{\varepsilon}_{j,t}^{ES}$ and $\underline{\varepsilon}_{j,t}^{ES}$ are a function of time. Indeed, when the vehicle leaves the home, its on-board batteries are no longer available and do not provide storage capacity to the system.

On the other hand, the individual storage limits necessary for (15) and (16) are easily calculable. Indeed, while the upper bound is given by the nominal capacity of devices, the lower one can be determined considering the depth-of-discharge characteristic of battery packs, as follows

$$\underline{\varepsilon}_{j}^{i} = \left(1 - \frac{\mathrm{DOD}_j^i}{100}\right) \cdot \bar{\varepsilon}_{j}^{i}; \forall j \in \mathcal{J} \wedge i \in \{Bat; EV\} \tag{17}$$

where DOD_j^i is the established depth-of-discharge of the i^{th} unit (stationary batteries or EV) of the j^{th} prosumer (in per unit).

Once each prosumer determines her storage limits by (15) and (16), they are communicated to the storage aggregator, who adds up them, as follows

$$\bar{\varepsilon}_{a,t}^{ES} = \sum_{j\in\mathcal{J}} \bar{\varepsilon}_{j,t}^{ES}\, , \underline{\varepsilon}_{a,t}^{ES} = \sum_{j\in\mathcal{J}} \underline{\varepsilon}_{j,t}^{ES}\, ; \forall t \in \mathcal{T} \tag{18}$$

The storage aggregator requires the maximum power dispatchable to storage units, similar to flexible appliances, which can be individually determined considering rated characteristics, as follows

$$\bar{p}_{j,t}^{ES} = \sum_{j\in\mathcal{J}} \bar{p}_{j}^{Bat} + \sum_{\substack{j\in\mathcal{J} \\ t\in\Theta_j^{EV}}} \bar{p}_{j}^{EV}\, ; \forall t \in \mathcal{T} \tag{19}$$

where $\bar{p}_{j}^{Bat}$ and $\bar{p}_{j}^{EV}$ are the rated power of stationary batteries and EV, respectively.

Again, it is worth noting that (19) accounts for the limited availability of EVs. While the charging/discharging power of EVs is limited by the capacity of chargers, the rated power of batteries can be determined as a function of their nominal capacity and the energy-to-power ratio [27], as said (20).

$$\bar{p}_{j}^{Bat} = \frac{\bar{\varepsilon}_{j}^{Bat}}{\mathrm{e2P}_j}; \forall j \in \mathcal{J} \tag{20}$$

where $\mathrm{e2P}_j$ is the nominal energy-to-power ratio of the batteries installed by the j^{th} prosumer (in hours).

Finally, each prosumer communicates the value obtained in (19) to the flexibility aggregator, who collects profiles in (21).

$$\bar{p}_{a,t}^{ES} = \sum_{j\in\mathcal{J}} \bar{p}_{j,t}^{ES}\, ; \forall t \in \mathcal{T} \tag{21}$$

2.3 - Day-ahead scheduling model

Throughout this section, the robust day-ahead scheduling model for the LEC described in Section 2.1 is derived. This task is assumed to be performed at the third layer by the community coordinator. In this sense, information from aggregators is treated as a parameter. This way, the community coordinator only receives aggregated information while individual profiles are not revealed, thus preserving the privacy of prosumers.

The day-ahead scheduling is determined over a daily time horizon, which is divided into $|\mathcal{T}|$ time intervals of size Δt. Note that this modelling allows us taking time intervals shorter than an hour, as usually. This adoption allows modelling fast power transitions, thus refining the scheduling results.

2.3.1 - Deterministic model

The deterministic day-ahead scheduling model in which uncertain parameters take expected values reads as

$$\min_{\boldsymbol{x},\boldsymbol{y}} \Delta t \cdot \sum_{t\in\mathcal{T}} \{\pi_t^{Import} \cdot p_t^{Import} - \pi_t^{Export} \cdot p_t^{Export}\} \tag{22a}$$

Subject to:

$$p_t^{Import} + p_{a,t}^{PV} + p_{a,t}^{ES,dch} = p_t^{Export} + \tilde{p}_{a,t}^{NF} + p_{a,t}^{F} + p_{a,t}^{ES,ch}; \forall t \in \mathcal{T} \tag{22b}$$

$$0 \le p_t^i \le y_t^i \cdot \overline{p}^i; \forall t \in \mathcal{T} \wedge i \in \{Import; Export\} \tag{22c}$$

$$y_t^{Import} + y_t^{Export} \le 1; \forall t \in \mathcal{T} \tag{22d}$$

$$0 \le p_{a,t}^{PV} \le \tilde{p}_{a,t}^{PV}; \forall t \in \mathcal{T} \tag{22e}$$

$$\tilde{\varepsilon}_a^F = \Delta t \cdot \sum_{t\in\mathcal{T}} p_{a,t}^F \tag{22f}$$

$$0 \le p_{a,t}^F \le \overline{p}_{a,t}^F; \forall t \in \mathcal{T} \tag{22g}$$

$$\varepsilon_{a,t}^{ES} = \varepsilon_{a,t-1}^{ES} - \varepsilon_{a,t-1}^{self-dch} + \Delta t \cdot \left(p_{a,t}^{ES,ch} \cdot \eta^{ES} - p_{a,t}^{ES,dch}/\eta^{ES}\right); \forall t \in \mathcal{T}\backslash t = 1 \tag{22h}$$

$$\varepsilon_{a,t}^{self-dch} = \bar{\varepsilon}_{a,t}^{ES} - \bar{\varepsilon}_{a,t+1}^{ES}; \forall t \in \mathcal{T}/t < |\mathcal{T}| \tag{22i}$$

$$\underline{\varepsilon}_{a,t}^{ES} \le \varepsilon_{a,t}^{ES} \le \bar{\varepsilon}_{a,t}^{ES}; \forall t \in \mathcal{T} \tag{22j}$$

$$\varepsilon_{a,1}^{ES} = \varepsilon_0^{ES} \cdot \bar{\varepsilon}_{a,1}^{ES}, \frac{\underline{\varepsilon}_{a,1}^{ES}}{\bar{\varepsilon}_{a,1}^{ES}} \le \varepsilon_0^{ES} \le 1 \tag{22k}$$

$$0 \le p_{a,t}^{ES,i} \le y_t^{ES,i} \cdot \bar{p}_{a,t}^{ES}; \forall t \in \mathcal{T} \wedge i \in \{ch; dch\} \tag{22l}$$

$$y_t^{ES,ch} + y_t^{ES,dch} \le 1; \forall t \in \mathcal{T} \tag{22m}$$

$$\boldsymbol{y} \in \{0,1\}; \forall t \in \mathcal{T} \tag{22n}$$

where $\boldsymbol{x}$ is the set of continuous variables (i.e. $\boldsymbol{x} = \left[p_t^{Import}, p_t^{Export}, p_{a,t}^{PV}, p_{a,t}^{ES,dch}, p_{a,t}^{ES,ch}, p_{a,t}^{F}, \varepsilon_{a,t}^{ES}\right]$, while $\boldsymbol{y}$ collects binary variables (i.e. $\boldsymbol{y} = \left[y_t^{Import}, y_t^{Export}, y_t^{ES,ch}, y_t^{ES,dch}\right]$). p_t^{Import} and p_t^{Export} the power imported and exported through the distribution network (trading with the local retailer), respectively at time t, while $p_{a,t}^{PV}$ stands for the instantaneous PV generation in the community at time t. Likewise, $p_{a,t}^{ES,dch}$ and $p_{a,t}^{ES,ch}$ are the power discharged and charged from storage systems at time t. On the other hand, $\varepsilon_{a,t}^{ES}$ denotes the total energy stored in storage systems at time t while binary variables indicate commitment statuses (e.g. $y_t^{ES,ch} = 1$ indicates that storage systems are on charging mode at time t).

The objective function (22a) comprises incomes/expenditures by exchanging energy with the local retailer. The set of constraints (22b)-(22n) describe a set of operational constraints that make the model feasible in real cases. In particular, (22b) is the power balance in the community, accounting for power exchanged with the retailer, local PV generation, storage systems as well as flexible and non-flexible demand. (22c) limits the power that can be exchanged with the distribution network through retailer trades, which is realistic assuming that power flow through branches is normally limited by either physical or contractual conditions, while (22d) avoids simultaneous imports and exports. The actual PV generation is considered controllable (not dispatchable) but limited to forecasted values in (22e). On the other hand, (22f) forces that energy required by the flexibility aggregator is fully satisfied respecting the maximum dispatchable power given in (22g).

In (22h), the dynamics of the storage aggregator are described, conceiving it as a cloud storage unit with estimated roundtrip efficiency [28]. In particular, (22h) includes the artificial self-discharge rate $\varepsilon_{a,t}^{self-dch}$ calculated in (22i), which accounts for the storage capacity loss due to departures of EVs. Indeed, this term is inserted in (22h) simulating an artificial energy consumption which models the departure of an EV at time t. (22j) expresses the limits in storage capacity, which are served as information by the storage aggregator. Since (22h) is not defined at the beginning of the scheduling horizon, the initial energy stored must be estimated. In this paper, this is done by establishing the parameter ε_0^{ES}. Thus, the operator can adopt conservative (low values of ε_0^{ES}) or optimistic (high values of ε_0^{ES}) strategies. Power dispatched through the storage operator is limited in (22l), taking into account the power limit informed by prosumers while simultaneous charge and discharge is avoided by imposing (22m). Finally, binary variables are described in (22n).

2.3.2 - Uncertainty modelling

In robust optimization, a proper representation of the uncertainty set is essential to obtain reliable results [22, 29]. In this paper, a polyhedral representation of the uncertainty set is considered, which typically presents good properties. This representation assumes that the actual realization of an uncertain parameter will lie within a given range. This modelling accepts adaptive settings by introducing the so-called uncertainty budget $0 \leq \Gamma \leq 1$. In particular, the polyhedral representation defines the behavior of an uncertain parameter d by the following expressions

$$d \in \left[\underline{d}, \overline{d}\right]; \forall d \tag{23a}$$

$$\left|\tilde{d} - d\right| \leq \Gamma \cdot \left(\overline{d} - \underline{d}\right); \forall d, 0 \leq \Gamma \leq 1 \tag{23b}$$

Note that (23) becomes deterministic if $\Gamma = 0$ forcing to $d = \tilde{d}$, whereas the complete range (23a) is considered if $\Gamma = 1$, which becomes (23) adaptable to different levels of robustness. The model (23) results nonlinear due to the absolute value in (23b). however, this nonlinearity is easily removable using the tricks described in [22]. Thus, the model (23) can be applied to the present problem (22) resulting in the set of additional constraints (24).

$$\sum_{t\in\mathcal{T}}\left\{\tilde{p}_{a,t}^{PV} - \hat{p}_{a,t}^{PV}\right\} \leq \Gamma \cdot \sum_{t\in\mathcal{T}} \tilde{p}_{a,t}^{PV} \tag{24a}$$

$$\hat{p}_{a,t}^{PV} \leq \tilde{p}_{a,t}^{PV}; \forall t \in \mathcal{T} \tag{24b}$$

$$\sum_{t\in\mathcal{T}}\left\{\hat{p}_{a,t}^{NF} - \tilde{p}_{a,t}^{NF}\right\} \leq \Gamma \cdot \sum_{t\in\mathcal{T}} \left\{\overline{p}_{a,t}^{NF} - \tilde{p}_{a,t}^{NF}\right\} \tag{24c}$$

$$\hat{\varepsilon}_a^F - \tilde{\varepsilon}_a^F \leq \Gamma \cdot \left(\overline{\varepsilon}_a^F - \tilde{\varepsilon}_a^F\right) \tag{24d}$$

In (24), three sources of uncertainties are considered. Firstly, the PV generation due to its dependence with weather parameters. Secondly, the non-flexible demand as it depends on unpredictable human behaviour. Thirdly, the energy demanded by flexible consumers as it depends on the ambient temperature.

2.3.3 - Robust bi-level problem

The robust counterpart of (22) casts as a bi-level framework which incorporates the uncertainty modelling (24), as follows

$$\max_{\substack{\hat{p}_{a,t}^{PV}, \hat{p}_{a,t}^{NF}, \hat{\varepsilon}_a^F; \\ \forall t \in \mathcal{T}}} \min_{\boldsymbol{x}, \boldsymbol{y}} \Delta t \cdot \sum_{t \in \mathcal{T}} \left\{ \pi_t^{Import} \cdot p_t^{Import} - \pi_t^{Export} \cdot p_t^{Export} \right\} \tag{25a}$$

Subject to:

$$p_t^{Import} + p_{a,t}^{PV} + p_{a,t}^{ES,dch} = p_t^{Export} + \hat{p}_{a,t}^{NF} + p_{a,t}^{F} + p_{a,t}^{ES,ch}; \forall t \in \mathcal{T} \tag{25b}$$

$$\hat{\varepsilon}_a^F = \Delta t \cdot \sum_{t \in \mathcal{T}} p_{a,t}^F \tag{25c}$$

(22c)-(22n) (25d)

Subject to:

(24a)-(24d) (25e)

$$p_{a,t}^{PV} \leq \hat{p}_{a,t}^{PV}; \forall t \in \mathcal{T} \tag{25f}$$

Firstly, it is worth noting that uncertain parameters in (22) were replaced by uncertain variables (denoted by tilde $\widehat{(\cdot)}$) in (25). This adoption allows considering uncertain parameters as variables, allowing them to vary within given intervals according to (24). (25) stands for a bi-level problem in which the inner problem is similar to (22), whereas the outer problem (max problem) seeks for the worst-case realization of uncertainties. Indeed, the outer problem takes the uncertain variables as decision space and seeks for maximizing the collective bill. It gives robust results assuming pessimistic realization of uncertainties. To this end, constraints (24) are incorporated in (25e). Declaring the uncertain parameters as variables require to replace the constraints (22b) and (22f) by (25b) and (25c), respectively, while the rest of constraints of the problem (22) are collected in (25d). On the other hand, (25f) is imposed to ensure that PV generation does not exceed the calculated PV potential.

This way, the problem (25) seeks the optimal scheduling plan for the LEC managing the variables $\boldsymbol{x}$ and $\boldsymbol{y}$ at the inner level, while the outer problem decides on the worst-case realization of uncertainties under the polyhedral representation given in (24).

Solving bi-level optimization problems is NP-hard [22], thus supposing a challenge for conventional solvers. To overcome this issue, the inner problem can be replaced by its Karush Kuhn Tucker (KKT) conditions and integrated within the outer one to convert the problem into a solvable single-level structure. However, only LP formulations are reducible to their KKT conditions, which is not possible for (25) due to the presence of binary variables. In the following sub-section, binary variables the presented problem are relaxed under plausible assumptions.

2.3.4 - Relaxing binary variables

Binary variables appear in (22) to model commitment statuses. In particular, these variables model the importing/exporting statuses of the LEC as well as the charging/discharging processes of batteries. Regarding batteries, different articles have already demonstrated that commitment statuses can be removed [30], since the cost minimization sense of the problem, together with a battery efficiency lower than 100 %, makes uneconomical the simultaneous charging and discharging of storage systems. Thus, this operational option would be likely discarded by the solver because its sub-optimality. One can easily check that these conditions meet in the presented problem and therefore the commitment statuses of batteries can be removed without any problem.

Regarding the importing/exporting status of the LEC, the same principle can be applied. In this case, it is assumed that exporting prices are always lower than purchasing ones. Note that this is a plausible assumption in power systems, where retailers typically offer lower selling prices in comparison with purchasing ones (e.g. see [31]).

Keeping the above in mind, the binary variables can be relaxed and thus they vanish from the problem, resulting in the following framework

$$\max_{\substack{\hat{p}^{PV}_{a,t}, \hat{p}^{NF}_{a,t}, \hat{\varepsilon}^{F}_{a}; \\ \forall t \in \mathcal{T}}} \min_{x} \Delta t \cdot \sum_{t \in \mathcal{T}} \left\{ \pi_t^{Import} \cdot p_t^{Import} - \delta \cdot \pi_t^{Import} \cdot p_t^{Export} \right\} \tag{26a}$$

Subject to:

$$p_t^{i} \leq \overline{p}^{i}; \forall t \in \mathcal{T} \wedge i \in \{Import; Export\} \tag{26b}$$

$$p_{a,t}^{ES,i} \leq \bar{p}_{a,t}^{ES}; \forall t \in \mathcal{T} \wedge i \in \{ch; dch\} \tag{26c}$$

(22e), (22g)-(22k), (25b), (25c) (26d)

Subject to:

(24a)-(24d), (25f) (26e)

In (26a), the selling price was replaced by $\delta \cdot \pi_t^{Import}$, with $\delta < 1$, thus ensuring that selling prices are lower than purchasing ones. On the other hand, (26b)-(26d) are the original constraints of (25) but omitting binary variables. Lastly, (26e) encompasses the uncertainty-related constraints. One can easily check that the inner problem in (26b)-(26d) is LP since binary variables vanished, and therefore can be replaced by its KKT conditions, which are detailed in the following sub-section.

2.3.5 - KKT conditions of (26b)-(26d)

KKT conditions of (26b)-(26d) are given below

$$\frac{\partial \mathcal{L}}{\partial p_t^{Import}} = \Delta t \cdot \pi_t^{Import} + \lambda_t^{(25b)} - \underline{\mu}_t^{(26b),Import} + \overline{\mu}_t^{(26b),Import} = 0; \forall t \in \mathcal{T} \tag{27a}$$

$$\frac{\partial \mathcal{L}}{\partial p_t^{Export}} = -\Delta t \cdot \delta \cdot \pi_t^{Import} - \lambda_t^{(25b)} - \underline{\mu}_t^{(26b),Export} + \overline{\mu}_t^{(26b),Export} = 0; \forall t \in \mathcal{T} \tag{27b}$$

$$\frac{\partial \mathcal{L}}{\partial p_{a,t}^{PV}} = \lambda_t^{(25b)} - \underline{\mu}_t^{(26e)} + \overline{\mu}_t^{(26e)} = 0; \forall t \in \mathcal{T} \tag{27c}$$

$$\frac{\partial \mathcal{L}}{\partial p_{a,t}^{F}} = -\lambda_t^{(25b)} + \Delta t \cdot \lambda^{(22f)} - \underline{\mu}_t^{(22g)} + \overline{\mu}_t^{(22g)} = 0; \forall t \in \mathcal{T} \tag{27d}$$

$$\frac{\partial \mathcal{L}}{\partial p_t^{ES,ch}} = -\lambda_t^{(25b)} - \Delta t \cdot \eta^{ES} \cdot \lambda_t^{(22h)} - \underline{\mu}_t^{(26c),ch} + \overline{\mu}_t^{(26c),ch} = 0; \forall t \in \mathcal{T} \tag{27e}$$

$$\frac{\partial \mathcal{L}}{\partial p_t^{ES,dch}} = \lambda_t^{(25b)} + \Delta t \cdot \frac{\lambda_t^{(22h)}}{\eta^{ES}} - \underline{\mu}_t^{(26c),dch} + \overline{\mu}_t^{(26c),dch} = 0; \forall t \in \mathcal{T} \tag{27f}$$

$$\frac{\partial \mathcal{L}}{\partial \varepsilon_{a,t}^{ES}} = \lambda_t^{(22h)} - \lambda_{t-1}^{(22h)} - \underline{\mu}_t^{(22j)} + \overline{\mu}_t^{(22j)} = 0; \forall t \in \mathcal{T} \backslash t = 1 \tag{27g}$$

$$\frac{\partial \mathcal{L}}{\partial \varepsilon_{a,1}^{ES}} = \lambda^{(22k)} - \underline{\mu}_1^{(22j)} + \overline{\mu}_1^{(22j)} = 0 \tag{27h}$$

$$0 \leq p_t^i \perp \underline{\mu}_t^{(26b),i} \geq 0; \forall t \in \mathcal{T} \wedge i \in \{Import; Export\} \tag{28a}$$

$$0 \leq \overline{p}^i - p_t^i \perp \overline{\mu}_t^{(26b),i} \geq 0; \forall t \in \mathcal{T} \wedge i \in \{Import; Export\} \tag{28b}$$

$$0 \leq p_{a,t}^{PV} \perp \underline{\mu}_t^{(22e)} \geq 0; \forall t \in \mathcal{T} \tag{28c}$$

$$0 \leq \hat{p}_{a,t}^{PV} - p_{a,t}^{PV} \perp \overline{\mu}_t^{(22e)} \geq 0; \forall t \in \mathcal{T} \tag{28d}$$

$$0 \leq p_{a,t}^{F} \perp \underline{\mu}_t^{(22g)} \geq 0; \forall t \in \mathcal{T} \tag{28e}$$

$$0 \leq \overline{p}_{a,t}^{F} - p_{a,t}^{F} \perp \overline{\mu}_t^{(22g)} \geq 0; \forall t \in \mathcal{T} \tag{28f}$$

$$0 \leq p_{a,t}^{ES,i} \perp \underline{\mu}_t^{(26c),i} \geq 0; \forall t \in \mathcal{T} \wedge i \in \{ch; dch\} \tag{28g}$$

$$0 \leq \bar{p}_{a,t}^{ES} - p_{a,t}^{ES,i} \perp \overline{\mu}_t^{(26c),i} \geq 0; \forall t \in \mathcal{T} \wedge i \in \{ch; dch\} \tag{28h}$$

$$0 \leq \varepsilon_{a,t}^{ES} - \underline{\varepsilon}_{a,t}^{ES} \perp \underline{\mu}_t^{(26j)} \geq 0; \forall t \in \mathcal{T} \tag{28g}$$

$$0 \leq \overline{\varepsilon}_{a,t}^{ES} - \varepsilon_{a,t}^{ES} \perp \overline{\mu}_t^{(26j)} \geq 0; \forall t \in \mathcal{T} \tag{28h}$$

where $\perp$ stands for complementarity while λ and μ are the dual variables of constraints in (22). In particular, the λ's link with equality constraints while the μ's are associated to inequality constraints. It is worth noting that inequality constraints in (22) are actually two constraints in most cases (e.g. (22c) can be decomposed into $0 \leq p_t^i$ and $p_t^i \leq y_t^i \cdot \overline{p}^i$). For these cases, the $\underline{\mu}$'s are linked to lower-bound constraints while the $\overline{\mu}$'s link with upper-bound constraints. Finally, superscripts in dual variables point out the constraint associated to (e.g. $\lambda_t^{(22h)}$ is linked to the constraint (22h)).

KKT conditions are formed by stationary (27) and complementarity (28) conditions. Stationary conditions (27) are associated to equality constraints and calculated by equalling to zero the Lagrangian function ($\mathcal{L}$) associated to (26). On the other hand, (28) represents the complementarity conditions arisen from the inequality constraints in (26). For more details about how KKT conditions are derived, the reader is referred to the seminars in [32].

2.3.6 - Final single-level robust optimization model

After replacing the inner problem (26b)-(26d) by its KKT conditions (27) and (28), it can be passed to the outer one resulting in the following single-level optimization framework

$$\max_{\substack{\boldsymbol{x}, \hat{p}_{a,t}^{PV}, \hat{p}_{a,t}^{NF}, \hat{\varepsilon}_{a}^{F}, \\ \underline{\boldsymbol{z}}, \overline{\boldsymbol{z}}, \boldsymbol{\lambda}, \underline{\boldsymbol{\mu}}, \overline{\boldsymbol{\mu}}; \forall t \in \mathcal{T}}} \Delta t \cdot \sum_{t \in \mathcal{T}} \left\{ \pi_t^{Import} \cdot p_t^{Import} - \delta \cdot \pi_t^{Import} \cdot p_t^{Export} \right\} \tag{29a}$$

Subject to:

(22h), (25b), (25c) (29b)

(27a)-(27h) (29c)

(28a)-(28h) (29d)

(26e) (29e)

$$\begin{cases} \boldsymbol{x} - \underline{\boldsymbol{x}} \leq \underline{\boldsymbol{z}} \cdot M \\ \underline{\boldsymbol{\mu}} \leq \left(1 - \underline{\boldsymbol{z}}\right) \cdot M \end{cases} \tag{29f}$$

$$\begin{cases} \overline{\boldsymbol{x}} - \boldsymbol{x} \leq \overline{\boldsymbol{z}} \cdot M \\ \overline{\boldsymbol{\mu}} \leq (1 - \overline{\boldsymbol{z}}) \cdot M \end{cases} \tag{29g}$$

$$\boldsymbol{\lambda}\text{: free} \tag{29h}$$

$$\underline{\boldsymbol{\mu}}, \overline{\boldsymbol{\mu}} \geq \boldsymbol{0} \tag{29i}$$

$$\underline{\boldsymbol{z}}, \overline{\boldsymbol{z}} \in \{0,1\} \tag{29j}$$

where $\boldsymbol{\lambda}$, $\underline{\boldsymbol{\mu}}$ and $\overline{\boldsymbol{\mu}}$ collect the λ's, $\underline{\mu}$'s and the $\overline{\mu}$'s, respectively, while $\underline{\boldsymbol{z}}$ and $\overline{\boldsymbol{z}}$ are binary variables introduced to linearize complementarity constraints.

In the problem above, (29b) are the equality constraints of the original problem which ensure its feasibility, while (29c) and (29d) collect the KKT conditions (27) and (28), respectively. On the other hand, (29e) stands for the uncertainty modelling (24). Note that (29f) and (29g) linearize the complementarity constraints using the disjunctive big-M method, as described in [33]. Lastly, (29h) declares the λ's free variables, the μ's are positive by (29i) and the z's are binary by (29j). It is worth noting that (29) is a MILP, for which a variety of commercial solvers is available.

2.4 - Case study

This section presents a case study with various numerical results in order to validate the developed aggregators models as well as exploring the role of each agent in LECs and how they are affected by the level of robustness. To this end, an experimental setup is constructed by coding the mathematical formulation presented in this paper in Matlab R2021a. The different optimization problems were solved using Gurobi [34], which offers free academia licenses currently. All the simulations were run on an Intel® Core™ i7-10700 K with 32.00 GB RAM over a 24 h time horizon with 15 minutes time resolution (96 time slots in total).

The results are presented for different number of prosumers, which results in different LEC sizes. The dataset for each prosumer regarding controllable appliances, PV panels, etc; was constructed randomly taking conventional data for this kind of installations (see Appendix). Nevertheless, weather parameters were considered identical for all the prosumers within the community due to they are expected to be located near each other. Thus, the expected solar irradiance and outdoor temperature are plotted in Fig. 2 (upper) and respond to real data at Madrid (Spain) in 2016 [35]. Using these data, the expected PV generation can be calculated using a suitable PV panel model [13]. As seen, these data correspond to hourly profiles over a daily basis and align with a typical day over the entire dataset. Note that the present paper focuses on day-ahead scheduling and therefore longer time horizons (monthly, yearly) are not relevant. Moreover, in order to provide illustrative results, weather parameters correspond to a day with significant PV production. This assumption allows to analyse the effect of renewable generators properly and thus validating the new tool (note that PV generation is actually one of the sources of uncertainty considered).

It is worth mentioning that days with less or almost null PV generation occur over a year (especially in winter). However, Nevertheless, as commented before, this paper focuses on day-ahead scheduling, which is performed daily and for which only the 24-h ahead are of interest. In addition, presenting results for each day of the year is unaffordable for a scientific paper and does not contribute with any additional information.

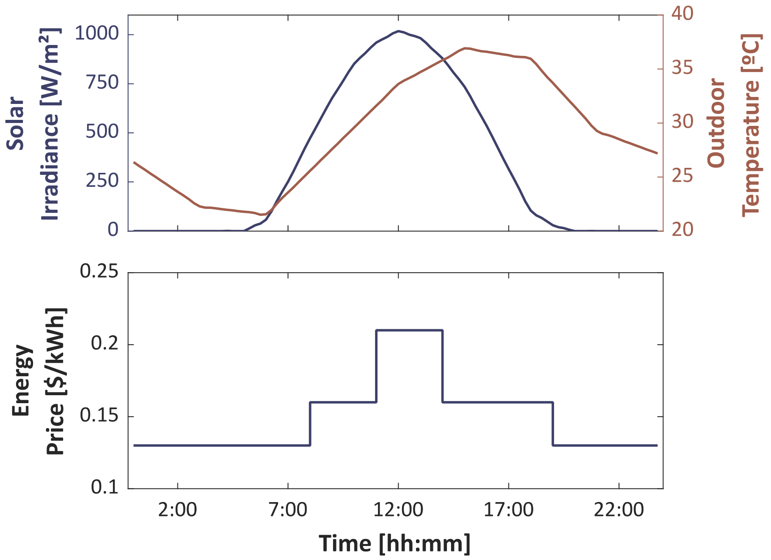

Fig. 2 - Expected weather parameters (upper) and retailer purchasing energy price (bottom)

It is assumed that a local retailer agrees with the community a three-period time-of-use tariff such as that showed in Fig. 2 (bottom), which corresponds with the 'One Luz 3 Periodos' currently offered by Endesa [36]. Regarding selling prices, $\delta = 0.9$ was taken, which is considered reasonable [37] and the retailer is assumed to limit at 10 kW the exchangeable power with the distribution network for each prosumer partaking in the community. Lastly, intervals for uncertain parameters were constructed by taking 20 % margin over expected profiles.

3 - Results and discussion

3.1 - Aggregated results

As commented previously, the aggregators constitute the second layer of the proposed LEC scheme. They serve as intermediate agents between the community coordinator and prosumers, avoiding to share with the former confidential information. In this sub-section, several indicative results are presented, which serve to validate the aggregators modelling presented in Section 2.2. Hence, the results presented in this section do not consider the effect of uncertainties, which will be explored in sub-sequent sections.

Fig. 3 plots the total non-flexible demand, PV potential and flexible demand for different number of prosumers. As expected, these indicators grow with the number of prosumers almost linearly, which indicates that the developed models represent fairly the prosumers' behaviour. Likewise, Fig. 4 plots the available storage margins. As seen in this figure, great storage capability is available at night due to the presence of EVs, which are still plugged at home. However, storage capability suddenly decreases at early morning, when most of vehicles depart. For the rest of the day, only stationary batteries are available to enable storage capability.

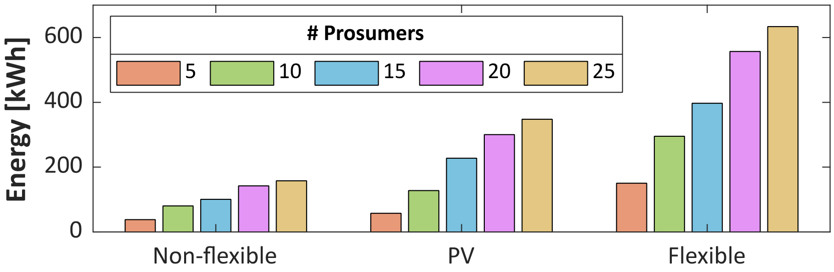

Fig. 3 - Aggregated energies for different number of prosumers

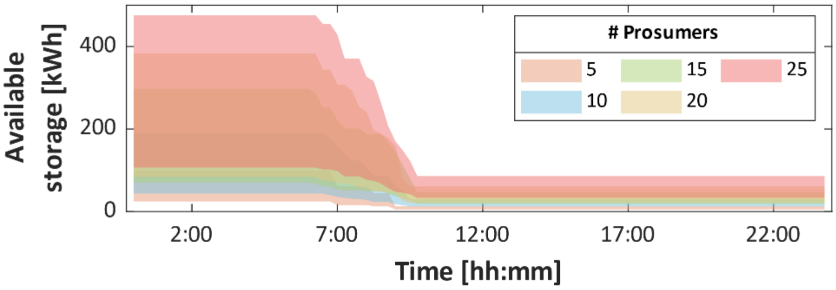

Fig. 4 - Available storage margins for different number of prosumers

On the other hand, Fig. 5 shows instantaneous net demand as well as schedulable flexible and storage power. Regarding net demand, it is clear that surplus energy is available at midday and afternoon, because high solar irradiance during these periods. At this time, the LEC becomes a net generator, being possible to share energy among prosumers and even sell energy to the grid. In contrast, prosumers demand energy during night to cover their own demand. Flexible demand is higher at midday and afternoon, assuming that most of prosumers are keen to schedule their controllable appliances at these time slots. Nevertheless, these devices can be shifted to other time instants, for convenience. Lastly, more power can be dispatched for storage systems at night, due to the presence of EVs, as previously mentioned.

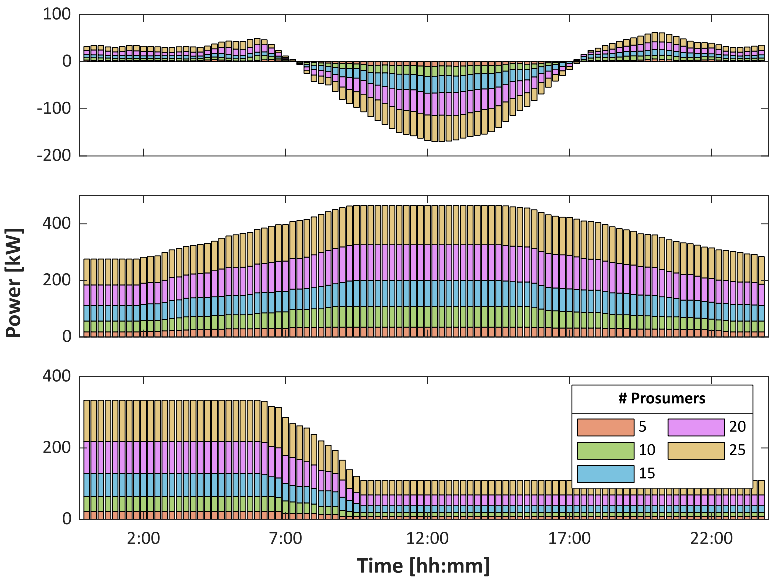

Fig. 5 - Expected net demand (upper) as well as dispatchable power for flexible devices (middle) and storage systems (bottom). In this figure, negative values indicate exportable power

3.2 - *Exploring the effect of adaptive robust scheduling*

3.2.1 - Impact on uncertain parameters

The possibility of setting the so-called uncertainty budget (Γ) gives adaptability to the proposed robust day-ahead scheduling model. To explore the effect of this parameter on uncertainties, Fig. 6 shows the assumed value of uncertain parameters for different levels of robustness. As expected, the different uncertainties evolve in a pessimistic way with the value of the uncertainty budget. Indeed, whereas demand-related parameters grow, the considered PV potential decrease.

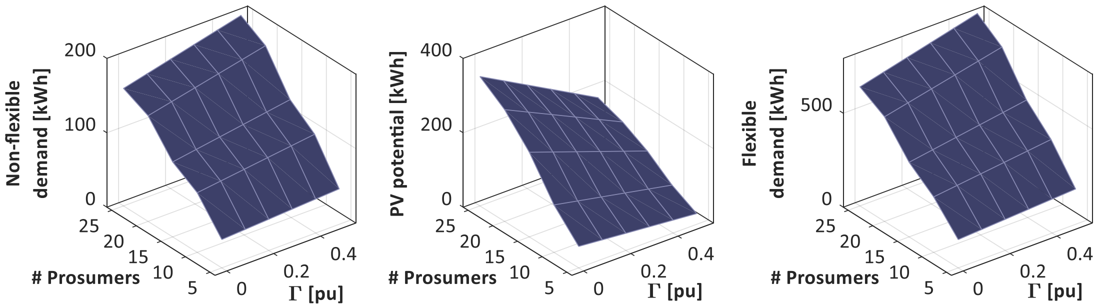

Fig. 6 - Assumed uncertain parameters for different levels of robustness and number of prosumers

The conditions drawn in Fig. 6 lead to a more stressful operability ambient, in which more demand has to be covered with limited renewable generation. To confirm this point, Fig. 7 plots the total energy imported by the studied LEC for different values of the uncertainty budget. As seen, the total energy imported increases with the value of Γ, as expected. In Fig. 7, it can be observed that the total energy imported increases with the number of prosumers, which further validates the developed model. In addition, the effect of the uncertainty budget on the imported energy is clearer as more prosumers partake in the community. Lastly, it is worth noting that more energy is imported in case of considering that storage units are few charged at the beginning of the time horizon ($\varepsilon_0^{ES} = 0.3$). This result is logic since, in case of being fully charged, storage systems can be leveraged to partially cover the community demand.

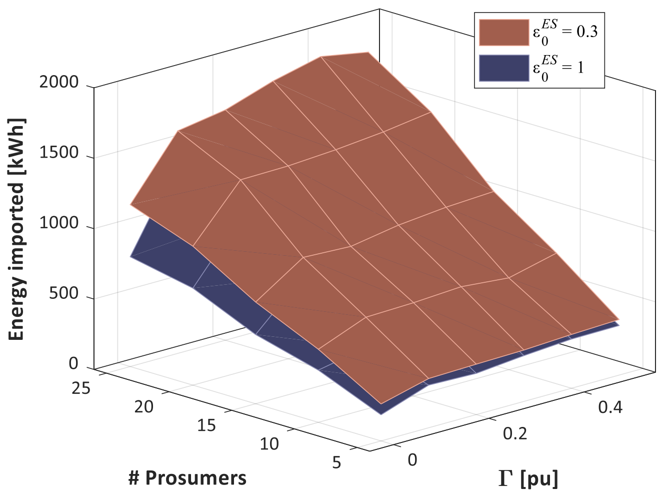

Fig. 7 - Total energy imported by the studied LEC for different levels of robustness and number of prosumers

3.2.2 - Impact on the collective bill

The stressful operating conditions described in the previous section should have a direct impact on the collective electricity bill. Indeed, Fig. 8 shows that the collective bill notably increases with the uncertainty budget. Actually, this fact is more noticeable as more prosumers partake in the community. In particular, the collective bill increased by 60 and 75 % with 5 and 25 prosumers, respectively. In Fig. 8 one can easily check that the collective expenditures were greater in case of $\varepsilon_0^{ES} = 0.3$, which was expected due to the unfavorable conditions observed in this scenario, as previously discussed. More specifically, the collective bill was approximately a 22 % higher in this scenario compared with $\varepsilon_0^{ES} = 1$.

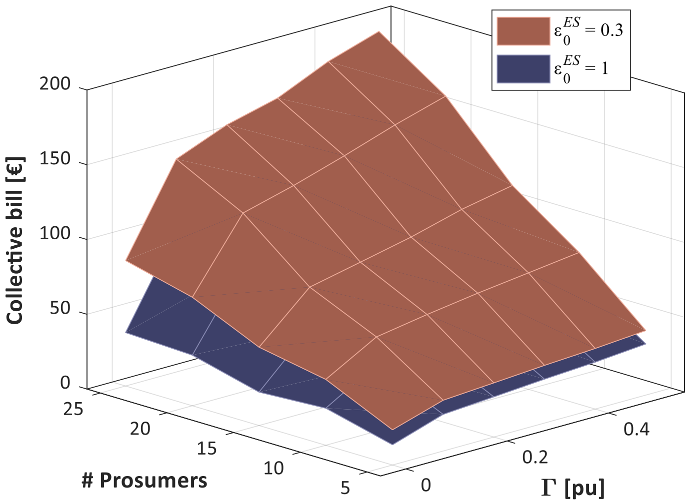

Fig. 8 - Collective bill for different levels of robustness and number of prosumers

The results in Fig. 8 show the monetary balance between the expenditures/incomes from exchanging energy with the network. Actually, selling energy is expected to be a primary activity in LECs, where eventual surplus renewable energy may help to alleviate the economy of prosumers. To get a better view at this point, Fig. 9 reports the monetary expenditures/incomes from purchasing/selling energy with the network. As observed, the cost of purchasing energy follows a similar trend to the collective bill, pointing out that this activity rules the overall cost of the community. However, incomes from exporting energy are not marginal and suppose an important monetary benefit for the entire community. Note that monetary results are more favourable with $\varepsilon_0^{ES} = 1$, due to the circumstances already mentioned. It is interesting to note that the incomes from selling energy increases with the number of prosumers, as expected. However, this index seems independent of the uncertainty budget. This surprising result will be further discussed in the following sub-section.

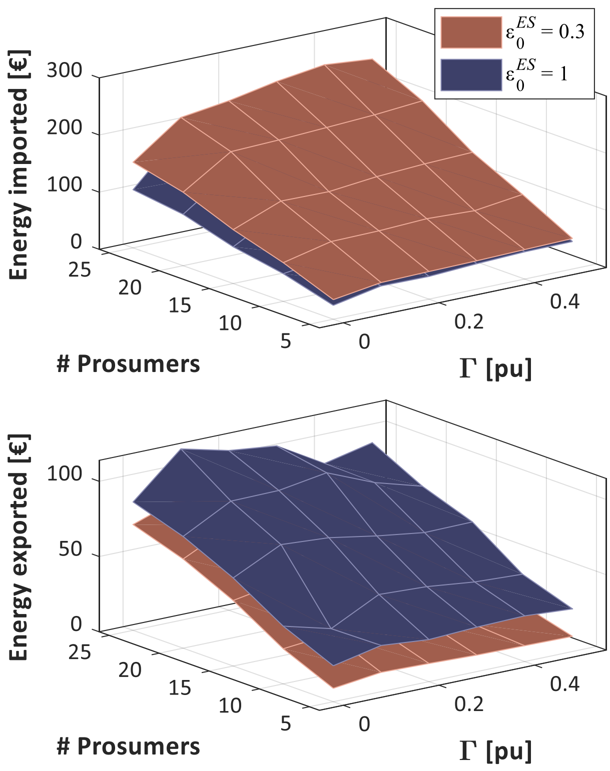

Fig. 9 - Monetary expenditures from purchasing energy (top) and incomes from selling energy (bottom) for different levels of robustness and number of prosumers

3.2.3 - Scheduling behaviour

To better understand some of the previous results, the scheduling behaviour of the community is now analysed (for the sake of simplicity, only results with $\varepsilon_0^{ES} = 1$ are shown in this section as similar conclusions can be drawn with $\varepsilon_0^{ES} = 0.3$). First, the net demand is shown in Fig. 10 for two extreme values of the uncertainty budget. In the deterministic case ($\Gamma = 0$), the net demand draws a logical behaviour, showing exportable power at midday and afternoon because high PV potential. However, in case of $\Gamma = 0.5$, the exported power during peak PV periods is limited, as expected, but more surprisingly a night exportable period appears at 5:00 h. This unexpected behaviour is propitiated by storage assets, which enable exporting energy through discharging process. Indeed, at this time most of EVs are plugged at home and therefore can be leveraged to export energy to the network and thus increasing the exportable capacity of the community. This same behaviour, although much more limited, is observed at 22:00 h, in this case through discharging stationary batteries.

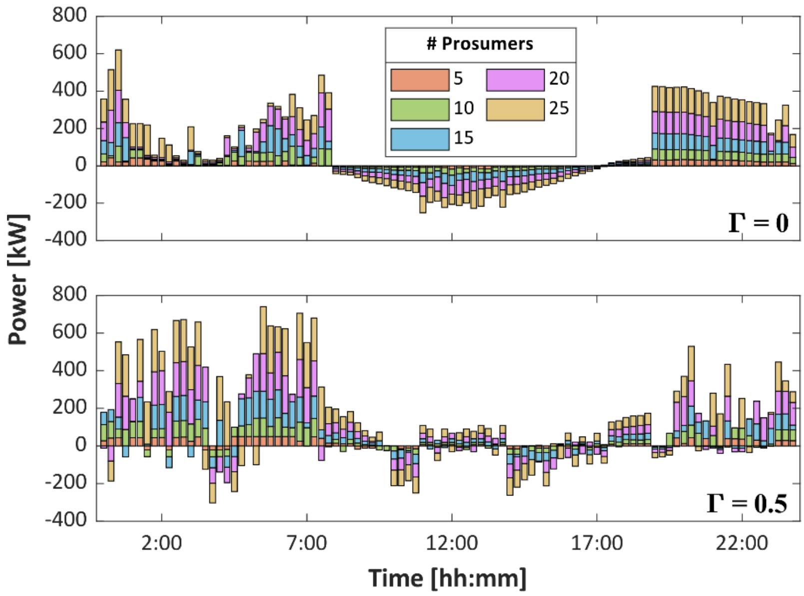

Fig. 10 - Net demand of the LEC under study for different number of prosumers. In this figure, negative values indicate exported power

Results in Fig. 10 reveal that under deterministic conditions the scheduling behaviour of the community is ruled by PV units, which ensure the most economic operation of the community. In contrast, when the operating strategy becomes risk-averse, limited PV generation is assumed and therefore the importance of PV units turns marginal. Under these unfavourable conditions, storage systems assume the leader role and the scheduling principle becomes oriented to these devices. To better illustrate this point, Fig. 11 shows the instantaneous aggregated energy stored in the LEC. As seen, in case of deterministic conditions, storage systems are partially discharged during night, when EVs are plugged, being practically ignored for the rest of the day. In contrast, clear discharging periods can be observed throughout the day in case of $\Gamma = 0.5$, thus showing that storage units (both stationary and on-board batteries) are much more profusely exploited under risk-averse conditions.

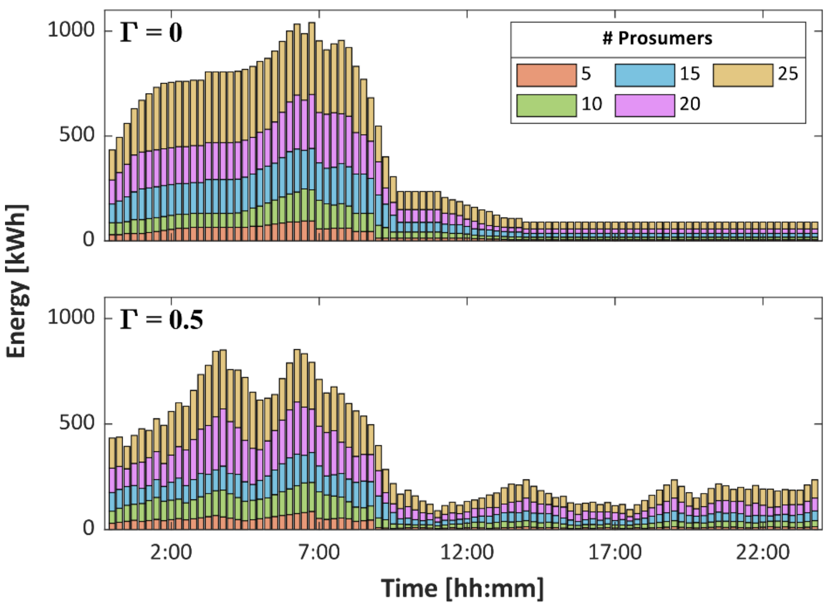

Fig. 11 - Instantaneous energy aggregator response for different number of prosumers

When storage systems start ruling the scheduling plan for the community, the rest of agents respond to them solidary. This is clear observed in Fig. 12, where the dispatched power to the flexibility aggregator is plotted. Under deterministic conditions, the community dispatches from 20:00 h, principally. At these time slots, net demand and energy price are low, thus supposing favourable conditions for scheduling flexible loads, while periods with high PV generation are leveraged for selling energy, as shown in Fig. 10. In contrast, most of the dispatched power is shifted to the beginning of the time horizon with $\Gamma = 0.5$. In this case, high storage capability during night propitiates more favourable conditions for flexibility dispatching.

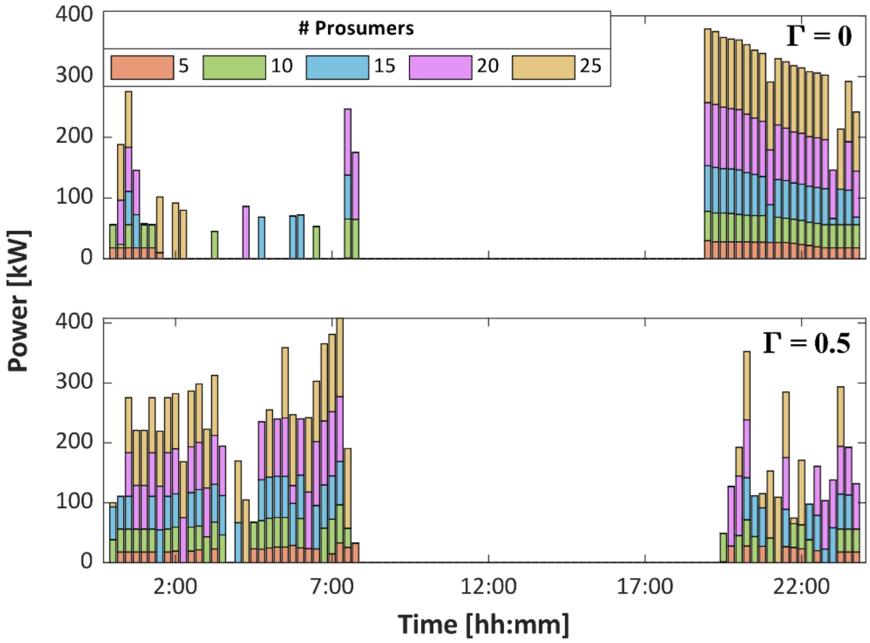

Fig. 12 - Instantaneous dispatched power to the flexibility aggregator for different number of prosumers

3.3 - Limitations

The developed model presents few limitations at mathematical level, as most frequent devices and functionalities in LECs have been developed. In this regard, storage (stationary and EVs), renewable generators, flexible demand and thermostatically-controlled appliances were included in the model and therefore the tool developed in this paper is considered functional and applicable to real cases. In this sense, the developed tool only presents assumable simplifications such as linearization of the thermal model of the building for modelling HVAC and EWH. In this sense, such simplification is justified in [38], demonstrating that the results obtained are perfectly comparable with those obtained with comprehensive models.

On the other hand, relaxing binary variables as explained in Section 2.3.4 requires that exporting prices were lower than importing ones. Although this assumption is typically observed in real cases, the developed model may fail if exporting and importing prices are equal. Nevertheless, the preliminary results obtained by the authors under such situation demonstrate that even so the developed mathematical model work well, as simultaneous imports and exports are normally naturally-discarded by the optimization solver.

The developed tool was tested in this work on a benchmark case study comprising real data. Nevertheless, its application in real installations should be studied in future works.

4 - Conclusions and future works

A novel LEC structure based on multiple aggregators has been presented in this work. This new paradigm stablishes a three-layer structure for energy communities wherein prosumers partake at first layer, while the coordinator takes decision at the third layer. The main merit of the proposed community structure is that a group of aggregators partake at the second layer, serving as a barrier between the coordinator and prosumers thus preserving their privacy. To this end, main features of prosumers are aggregated so that the coordinator only receives aggregated information instead of individual data.

A robust day-ahead scheduling model for the proposed community structure has been also proposed. The new model is based on. To this end, source of uncertainties in energy communities were modelled as polyhedral uncertainty sets and the overall optimization model was formulated as a bi-level structure that can be reduced to a single-level framework, and is formulated as a MILP, being in consequence solvable by a variety of off-the-shelf solvers.

A benchmark case study was conducted to validate the new tool. Firstly, the effect of aggregation was highlighted, validating the new aggregators' models developed in this paper. The rest of results focused on scheduling, economic and energy results. It was shown that the proposed robust methodology worked well in the presented case study, assuming pessimistic evolution of uncertainties following the value of the so-called uncertainty level. Other results showed the impact of robustness on economic indicators. In particular, the impact of adaptive robustness was analysed, showing that collective bill can be incremented by 75 % if risk-averse conditions are assumed. Other relevant results and particular behaviour have been also identified, for example, it was highlighted that the scheduling plan for the community is ruled by storage assets rather than PV generators when pessimistic values of uncertainties are considered.

In future research, the developed mathematical modelling can be adapted to other energy structures wherein privacy concerns, such as microgrids and distribution networks. Moreover, the developed robust model can be further applied to smart grids. Future works should be also focused on further analysing the role of storage assets in LECs and propose novel tools to exploit optimally this kind of devices.

Appendix - Prosumers data

Below, the ranges considered for constructing the dataset of each prosumer in the case study of Section 2.4 are reported.

- PV peak power $\in [1, 4]\ kW$
- Number of controllable appliances $\in [0, 3]$
- Duty cycle of each controllable appliance $\in [2, 6]\ hours$
- Rated power of each controllable appliance $\in [0.5, 2]\ kW$
- Time window of each controllable appliance $\in [2{:}\,00\ h, 23{:}\,45\ h]$
- Battery capacity $\in [1, 5]\ kWh$
- Battery depth-of-discharge $\in [40, 80]\ \%$
- Battery rated power $\in [0.6, 3.3]\ kW$

- Battery efficiency $= 95\ \%$
- HVAC rated power $\in [1.5, 2]\ kW$
- HVAC setpoint $\in [23, 25]$ °C
- HVAC dead-band $\in [0.5, 1.5]$ °C
- HVAC coefficient-of-performance $\in [1, 2]$
- $A_j^{Air,in} \in [4.8, 8]$
- $B_j^{Air,in} \in [0.42, 0.7]$
- EV total capacity $\in [10, 22]\ kWh$
- EV initial state-of-charge $\in [0.4, 0.8]$ of the total capacity
- EV total capacity $\in [10, 22]\ kWh$
- EV charging rated power $= 3\ kW$
- EV departure time $\in [6{:}00\ h, 9{:}30\ h]$

It is worth noting that non-flexible demand for each prosumer was taken randomly from the dataset available in [39], whose daily hourly data is plotted in Fig. A1 (upper). On the other hand, hot water consumption was set randomly from conventional consumption patterns plotted in Fig. A1 (bottom), while data regarding EWHs were taken from [40].

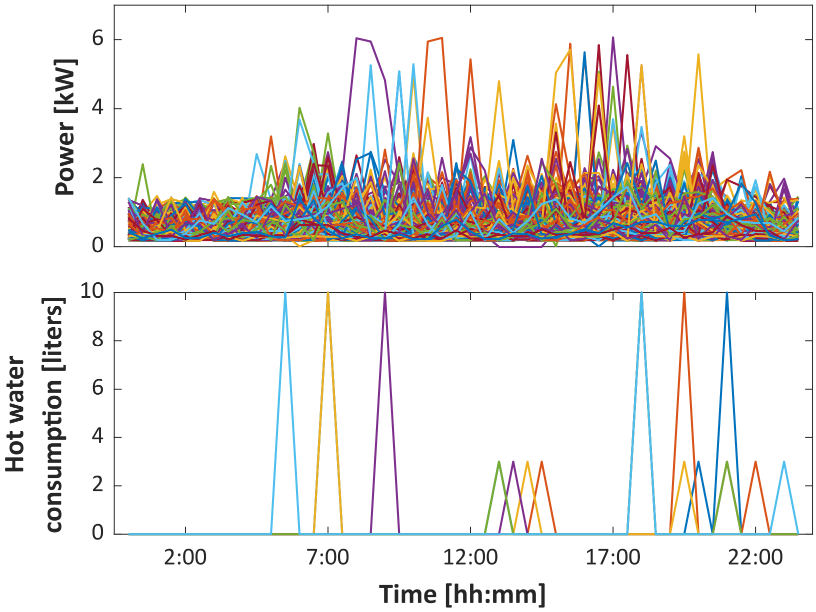

Fig. A1 - Non-flexible demand (upper) and hot water consumption (bottom) scenarios considered for building prosumers' datasets

References

[1] G. Aydin. The Modeling of Coal-related CO_2 Emissions and Projections into Future Planning. *Energy Sources, Part A: Recovery, Utilization, and Environmental Effects* 2014; 36(2): 191-201. https://doi.org/10.1080/15567036.2012.760018.

[2] G. Aydin. Production Modeling in the Oil and Natural Gas Industry: An Application of Trend Analysis. *Petroleum Science and Technology* 2014; 32(5): 555-64. https://doi.org/10.1080/10916466.2013.825271.

[3] C. Feng, Z. Li, M. Shahidehpour, F. Wen, W. Liu, X. Wang. Decentralized Short-Term Voltage Control in Active Power Distribution Systems. *IEEE Transactions on Smart Grid* 2018; 9(5): 4566-76. https://doi.org/10.1109/TSG.2017.2663432.

[4] U.S. Department of Energy. Confronting the Duck Curve: How to Address Over-Generation of Solar Energy. Online, available at: https://www.energy.gov/eere/articles/confronting-duck-curve-how-address-over-generation-solar-energy, (accessed on Mar. 17, 2023).

[5] European Commission. Energy communities. Online, available at: https://energy.ec.europa.eu/topics/markets-and-consumers/energy-communities_en, (accessed on Mar. 17, 2023).

[6] B.P. Koirala, E. Koliou, J. Friege, R.A. Hakvoort, P.M. Herder. Energetic communities for community energy: A review of key issues and trends shaping integrated community energy systems. *Renewable and Sustainable Energy Reviews* 2016; 56: 722-44. https://doi.org/10.1016/j.rser.2015.11.080.

[7] N. Vespermann, T. Hamacher, J. Kazempour. Risk Trading in Energy Communities. *IEEE Transactions on Smart Grid* 2021; 12(2): 1249-63. https://doi.org/10.1109/TSG.2020.3030319.

[8] A. Fazeli, M. Sumner, C.M. Johnson, E. Christopher. Coordinated optimal dispatch of distributed energy resources within a smart energy community cell. In: *2012 3rd IEEE PES Innovative Smart Grid Technologies Europe (ISGT Europe)*; Berlin, Germany, 2012: 1-10. https://doi.org/10.1109/ISGTEurope.2012.6465812.

[9] M. Steinheimer, U. Trick, P. Ruhrig. Energy communities in Smart Markets for optimisation of peer-to-peer interconnected Smart Homes. In: *2012 8th International Symposium on Communication Systems, Networks & Digital Signal Processing (CSNDSP)*; Poznan, Poland, 2012: 1-6. https://doi.org/10.1109/CSNDSP.2012.6292732.

[10] M. Khorasany, R. Razzaghi, A.S. Gazafroudi. Two-stage mechanism design for energy trading of strategic agents in energy communities. *Applied Energy* 2021; 295: 117036. https://doi.org/10.1016/j.apenergy.2021.117036.

[11] A.D. Mustika, R. Rigo-Mariani, V. Debusschere, A. Pachurka. A two-stage management strategy for the optimal operation and billing in an energy community with collective self-consumption. *Applied Energy* 2022; 310: 118484. https://doi.org/10.1016/j.apenergy.2021.118484.

[12] M.S. Javadi, M. Gough, A.E. Nezhad, S.F. Santos, M. Shafie-khah, J.P.S. Catalão. Pool trading model within a local energy community considering flexible loads, photovoltaic generation and energy storage systems. *Sustainable Cities and Society* 2022; 79: 103747. https://doi.org/10.1016/j.scs.2022.103747.

[13] M. Tostado-Véliz, S. Kamel, H.M. Hasanien, R.A. Turky, F. Jurado. Optimal energy management of cooperative energy communities considering flexible demand, storage and vehicle-to-grid under uncertainties. *Sustainable Cities and Society* 2022; 84: 104019. https://doi.org/10.1016/j.scs.2022.104019.

[14] M. Tostado-Véliz, A.R. Jordehi, S.A. Mansouri, F. Jurado. A two-stage IGDT-stochastic model for optimal scheduling of energy communities with intelligent parking lots. *Energy* 2023; 263(D): 126018. https://doi.org/10.1016/j.energy.2022.126018.

[15] M. Tostado-Véliz, S.A. Mansouri, A. Rezaee-Jordehi, D. Icaza-Alvarez, F. Jurado. Information Gap Decision Theory-based day-ahead scheduling of energy communities with collective hydrogen chain. *International Journal of Hydrogen Energy* 2023; 48(20): 7154-69. https://doi.org/10.1016/j.ijhydene.2022.11.183.

[16] C. Feng, F. Wen, S. You, Z. Li, F. Shahnia, M. Shahidehpour. Coalitional Game-Based Transactive Energy Management in Local Energy Communities. *IEEE Transactions on Power Systems* 2020; 35(3): 1729-40. https://doi.org/10.1109/TPWRS.2019.2957537.

[17] H.-C. Jo, G. Byeon, J.-Y. Kim, S.-K. Kim. Optimal Scheduling for a Zero Net Energy Community Microgrid With Customer-Owned Energy Storage Systems. *IEEE Transactions on Power Systems* 2021; 36(3): 2273-80. https://doi.org/10.1109/TPWRS.2020.3036077.

[18] S. Lilla, C. Orozco, A. Borghetti, F. Napolitano, F. Tossani. Day-Ahead Scheduling of a Local Energy Community: An Alternating Direction Method of Multipliers Approach. *IEEE Transactions on Power Systems* 2020; 35(2): 1132-42. https://doi.org/10.1109/TPWRS.2019.2944541.

[19] C. Orozco, A. Borghetti, B. De Schutter, F. Napolitano, G. Pulazza, F. Tossani. Intra-day scheduling of a local energy community coordinated with day-ahead multistage decisions.

Sustainable Energy, Grids and Networks 2022; 29: 100573. https://doi.org/10.1016/j.segan.2021.100573.

[20] H. Nagpal, I.-I. Avramidis, F. Capitanescu, A.G. Madureira. Local Energy Communities in Service of Sustainability and Grid Flexibility Provision: Hierarchical Management of Shared Energy Storage. *IEEE Transactions on Sustainable Energy* 2022; 13(3): 1523-35. https://doi.org/10.1109/TSTE.2022.3157193.

[21] L.A. Roald, D. Pozo, A. Papavasiliou, D.K. Molzahn, J. Kazempour, A. Conejo. Power systems optimization under uncertainty: A review of methods and applications. *Electric Power Systems Research* 2023; 214(A): 108725. https://doi.org/10.1016/j.epsr.2022.108725.

[22] C. Ruiz, A.J. Conejo. Robust transmission expansion planning. *European Journal of Operational Research* 2015; 242(2): 390-401. https://doi.org/10.1016/j.ejor.2014.10.030.

[23] I. Riepin, M. Schmidt, L. Baringo, F. Müsgens. Adaptive robust optimization for European strategic gas infrastructure planning. *Applied Energy* 2022; 324: 119686. https://doi.org/10.1016/j.apenergy.2022.119686.

[24] M. Tostado-Véliz, S. Kamel, F. Aymen, F. Jurado. A novel hybrid lexicographic-IGDT methodology for robust multi-objective solution of home energy management systems. *Energy* 2022; 253: 124146. https://doi.org/10.1016/j.energy.2022.124146.

[25] M. Shafie-Khah, P. Siano. A Stochastic Home Energy Management System Considering Satisfaction Cost and Response Fatigue. *IEEE Transactions on Industrial Informatics* 2018; 14(2): 629-38. https://doi.org/10.1109/TII.2017.2728803.

[26] N.G. Paterakis, O. Erdinç, A.G. Bakirtzis, J.P.S. Catalão. Optimal Household Appliances Scheduling Under Day-Ahead Pricing and Load-Shaping Demand Response Strategies. *IEEE Transactions on Industrial Informatics* 2015; 11(6): 1509-19. https://doi.org/10.1109/TII.2015.2438534.

[27] I. Alsaidan, A. Khodaei, W. Gao. A Comprehensive Battery Energy Storage Optimal Sizing Model for Microgrid Applications. *IEEE Transactions on Power Systems* 2018; 33(4): 3968-80. https://doi.org/10.1109/TPWRS.2017.2769639.

[28] Z. Liu, J. Yang, W.Z. Song, N. Xue, S. Li, M. Fang. Research on cloud energy storage service in residential microgrids. *IET Renewable Power Generation* 2019; 13(16): 3097-105. https://doi.org/10.1049/iet-rpg.2019.0464.

[29] J.S. Giraldo, J.A. Castrillon, J.C. López, M.J. Rider, C.A. Castro. Microgrids Energy Management Using Robust Convex Programming. *IEEE Transactions on Smart Grid* 2019; 10(4): 4520-30. https://doi.org/10.1109/TSG.2018.2863049.

[30] S. Sarfarazi, S. Mohammadi, D. Khastieva, M.R. Hesamzadeh, V. Bertsch, D. Bunn. An optimal real-time pricing strategy for aggregating distributed generation and battery storage systems in energy communities: A stochastic bilevel optimization approach. *International Journal of Electrical Power & Energy Systems* 2023; 147: 108770. https://doi.org/10.1016/j.ijepes.2022.108770.

[31] Endesa. Solar Simply Tariff. Online, available at: https://www.endesa.com/en/catalog/light/tempo/self-consumption-tariff-with-solar-surplus-simply, (accessed on Apr. 12, 2023).

[32] J. Kazempour. Advanced Optimization and Game Theory for Energy Systems. Online, available at: https://www.jalalkazempour.com/teaching, (accessed on Jan. 10, 2024).

[33] M. Tostado-Véliz, H.M. Hasanien, A.R. Jordehi, R.A. Turky, F. Jurado. Risk-averse optimal participation of a DR-intensive microgrid in competitive clusters considering response fatigue. *Applied Energy* 2023; 339: 120960. https://doi.org/10.1016/j.apenergy.2023.120960.

[34] Gurobi Optimization L.L.C. Gurobi Optimizer Reference Manual, 2021. Online, available at: https://www.gurobi.com, (accessed on Apr. 12, 2023).

[35] Endesa. One Luz 3 Periodos Tariff. Online, available at: https://www.endesa.com/en/catalog/light/one/tarifa-one-luz-3periodos-en, (accessed on Apr. 12, 2023).

[36] European Comission. Photovoltaic Geographical Information System. Online, available at: https://re.jrc.ec.europa.eu/pvg_tools/en/tools.html, (accessed on Apr. 12, 2023).

[37] M.S. Javadi, M. Lotfi, A.E. Nezhad, A. Anvari-Moghaddam, J.M. Guerrero, J.P.S. Catalão. Optimal Operation of Energy Hubs Considering Uncertainties and Different Time Resolutions.

IEEE Transactions on Industry Applications 2020; 56(5): 5543-52. https://doi.org/10.1109/TIA.2020.3000707.

[38] Haiming Wang et al. Demand response through smart home energy management using thermal inertia. In: *2013 Australasian Universities Power Engineering Conference (AUPEC)*; Hobart, TAS, Australia, 2013: 1-6. https://doi.org/10.1109/AUPEC.2013.6725442.

[39] T. Singh. Smart Home Dataset with weather Information. Online, available at: https://www.kaggle.com/datasets/taranvee/smart-home-dataset-with-weather-information, (accessed on Apr. 12, 2023).

[40] M. Tostado-Véliz, A.R. Jordehi, D. Icaza, S.A. Mansouri, F. Jurado. Optimal participation of prosumers in energy communities through a novel stochastic-robust day-ahead scheduling model. *International Journal of Electrical Power & Energy Systems* 2023; 147: 108854. https://doi.org/10.1016/j.ijepes.2022.108854.